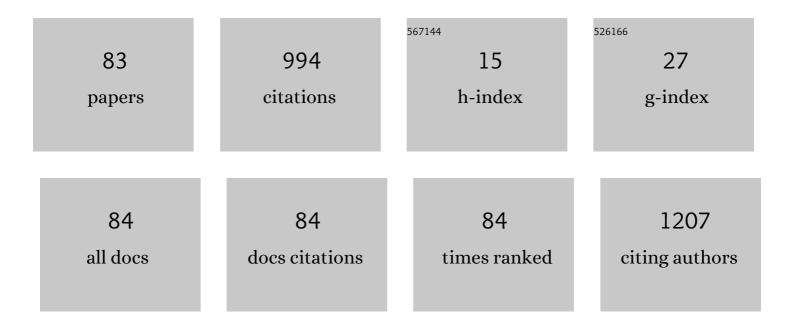
List of Publications by Year in descending order

Source: https://exaly.com/author-pdf/449129/publications.pdf Version: 2024-02-01



ARDOLDEZA SAEADI

#	Article	IF	CITATIONS
1	Anomaly Detection in Hyperspectral Images Based on an Adaptive Support Vector Method. IEEE Geoscience and Remote Sensing Letters, 2011, 8, 646-650.	1.4	117
2	Object-based classification of hyperspectral data using Random Forest algorithm. Geo-Spatial Information Science, 2018, 21, 127-138.	2.4	68
3	An Approach for Subpixel Anomaly Detection in Hyperspectral Images. IEEE Journal of Selected Topics in Applied Earth Observations and Remote Sensing, 2013, 6, 769-778.	2.3	59
4	A COMPARISON STUDY OF DIFFERENT KERNEL FUNCTIONS FOR SVM-BASED CLASSIFICATION OF MULTI-TEMPORAL POLARIMETRY SAR DATA. International Archives of the Photogrammetry, Remote Sensing and Spatial Information Sciences - ISPRS Archives, 0, XL-2/W3, 281-285.	0.2	54
5	An Improved FCM Algorithm Based on the SVDD for Unsupervised Hyperspectral Data Classification. IEEE Journal of Selected Topics in Applied Earth Observations and Remote Sensing, 2013, 6, 831-839.	2.3	46
6	Large-Scale Total Water Storage and Water Flux Changes over the Arid and Semiarid Parts of the Middle East from GRACE and Reanalysis Products. Surveys in Geophysics, 2017, 38, 591-615.	2.1	45
7	Comparing multi-objective optimization techniques to calibrate a conceptual hydrological model using in situ runoff and daily GRACE data. Computational Geosciences, 2018, 22, 789-814.	1.2	41
8	Multiple Kernel Learning for Remote Sensing Image Classification. IEEE Transactions on Geoscience and Remote Sensing, 2018, 56, 1425-1443.	2.7	36
9	Improving the SVDD Approach to Hyperspectral Image Classification. IEEE Geoscience and Remote Sensing Letters, 2012, 9, 594-598.	1.4	29
10	Global height datum unification: a new approach in gravity potential space. Journal of Geodesy, 2005, 79, 512-523.	1.6	25
11	Hybrid SAR Speckle Reduction Using Complex Wavelet Shrinkage and Non-Local PCA-Based Filtering. IEEE Journal of Selected Topics in Applied Earth Observations and Remote Sensing, 2019, 12, 1489-1496.	2.3	24
12	Semi-supervised classification of hyperspectral image using random forest algorithm. , 2014, , .		23
13	Enhanced decision tree ensembles for land-cover mapping from fully polarimetric SAR data. International Journal of Remote Sensing, 2017, 38, 7138-7160.	1.3	23
14	A Hybrid Kernel-Based Change Detection Method for Remotely Sensed Data in a Similarity Space. Remote Sensing, 2015, 7, 12829-12858.	1.8	20
15	Crop biomass estimation using multi regression analysis and neural networks from multitemporal L-band polarimetric synthetic aperture radar data. International Journal of Remote Sensing, 2019, 40, 6822-6840.	1.3	20
16	Mapping urban land cover based on spatial-spectral classification of hyperspectral remote-sensing data. International Journal of Remote Sensing, 2016, 37, 440-454.	1.3	16
17	Deep Learning-Based Estimation of Crop Biophysical Parameters Using Multi-Source and Multi-Temporal Remote Sensing Observations. Agronomy, 2021, 11, 1363.	1.3	16
18	A Novel Multiple Kernel Learning Framework for Multiple Feature Classification. IEEE Journal of Selected Topics in Applied Earth Observations and Remote Sensing, 2017, 10, 3734-3743.	2.3	15

#	Article	IF	CITATIONS
19	MSMD: maximum separability and minimum dependency feature selection for cropland classification from optical and radar data. International Journal of Remote Sensing, 2018, 39, 2159-2176.	1.3	15
20	A GA-Based Multi-View, Multi-Learner Active Learning Framework for Hyperspectral Image Classification. Remote Sensing, 2020, 12, 297.	1.8	15
21	A new ellipsoidal gravimetric, satellite altimetry and astronomic boundary value problem, a case study: The geoid of Iran. Journal of Geodynamics, 2005, 39, 545-568.	0.7	14
22	Similarity-Based Multiple Kernel Learning Algorithms for Classification of Remotely Sensed Images. IEEE Journal of Selected Topics in Applied Earth Observations and Remote Sensing, 2017, 10, 2012-2021.	2.3	13
23	A New Convolutional Kernel Classifier for Hyperspectral Image Classification. IEEE Journal of Selected Topics in Applied Earth Observations and Remote Sensing, 2021, 14, 11240-11256.	2.3	12
24	Multi-temporal full polarimetry L-band SAR data classification for agriculture land cover mapping. , 2014, , .		11
25	Spectral–Spatial Semisupervised Hyperspectral Classification Using Adaptive Neighborhood. IEEE Journal of Selected Topics in Applied Earth Observations and Remote Sensing, 2017, 10, 4183-4197.	2.3	11
26	Particle swarm optimization of kernel-based fuzzy c-means for hyperspectral data clustering. Journal of Applied Remote Sensing, 2012, 6, 063601.	0.6	9
27	Environmental monitoring based on automatic change detection from remotely sensed data: kernel-based approach. Journal of Applied Remote Sensing, 2015, 9, 095992.	0.6	9
28	Fast approximation algorithm to noise components estimation in long-term GPS coordinate time series. Journal of Geodesy, 2021, 95, 1.	1.6	9
29	Ellipsoidal terrain correction based on multi-cylindrical equal-area map projection of the reference ellipsoid. Journal of Geodesy, 2004, 78, 114.	1.6	8
30	A new approach for land surface emissivity estimation using LDCM data in semi-arid areas: exploitation of the ASTER spectral library data set. International Journal of Remote Sensing, 2016, 37, 5060-5085.	1.3	8
31	IRG2016: RBF-based regional geoid model of Iran. Studia Geophysica Et Geodaetica, 2018, 62, 380-407.	0.3	8
32	An auto-encoder based classifier for crop mapping from multitemporal multispectral imagery. International Journal of Remote Sensing, 2021, 42, 986-1016.	1.3	8
33	Evaluation of different gravimetric methods to Moho recovery in Iran. Annals of Geophysics, 2019, 62,	0.5	8
34	Harmonic analysis of the ionospheric electron densities retrieved from FORMOSAT-3/COSMIC radio occultation measurements. Advances in Space Research, 2012, 49, 1520-1528.	1.2	7
35	Fusion Methods for Land Surface Emissivity and Temperature Retrieval of the Landsat Data Continuity Mission Data. IEEE Transactions on Geoscience and Remote Sensing, 2016, 54, 3842-3855.	2.7	7
36	Local gravity field modeling using spherical radial basis functions and a genetic algorithm. Comptes Rendus - Geoscience, 2017, 349, 106-113.	0.4	7

#	Article	IF	CITATIONS
37	LOCAL EVALUATION OF EARTH GRAVITATIONAL MODELS, CASE STUDY: IRAN. Geodesy and Cartography, 2017, 43, 1-13.	0.2	7
38	Application of Radial Basis Functions for Height Datum Unification. Geosciences (Switzerland), 2018, 8, 369.	1.0	7
39	Fast collocation for Moho estimation from GOCE gravity data: the Iran case study. Geophysical Journal International, 2020, 221, 651-664.	1.0	7
40	New Cylindrical Equal Area and Conformal Map Projections of the Reference Ellipsoid for Local Applications. Survey Review, 2007, 39, 132-144.	0.7	6
41	Determining the Gravitational Gradient Tensor Using Satellite-Altimetry Observations over the Persian Gulf. Marine Geodesy, 2014, 37, 404-418.	0.9	6
42	Application of the RTM-technique to gravity reduction for tracking near-surface mass-density anomalies: A case study of salt diapirs in Iran. Studia Geophysica Et Geodaetica, 2015, 59, 409-423.	0.3	6
43	A comparative study on Multiple Kernel Learning for remote sensing image classification. , 2016, , .		5
44	A numerically efficient technique of regional gravity field modeling using Radial Basis Functions. Comptes Rendus - Geoscience, 2016, 348, 99-105.	0.4	5
45	Natural hazard damage detection based on object-level support vector data description of optical and SAR Earth observations. International Journal of Remote Sensing, 2017, 38, 3356-3374.	1.3	5
46	The effect of soil salinity on the use of the universal triangle method to estimate saline soil moisture from Landsat data: application to the SMAPEx-2 and SMAPEx-3 campaigns. International Journal of Remote Sensing, 2017, 38, 6623-6652.	1.3	5
47	Separability analysis of multifrequency SAR polarimetric features for land cover classification. Remote Sensing Letters, 2017, 8, 1152-1161.	0.6	5
48	Multiple kernel representation and classification of multivariate satellite-image time-series for crop mapping. International Journal of Remote Sensing, 2018, 39, 149-168.	1.3	5
49	Gaussian mixture model and Markov random fields for hyperspectral image classification. European Journal of Remote Sensing, 2018, 51, 889-900.	1.7	5
50	Multiple classifier systems for classification of multifrequency PolSAR images with limited training samples. International Journal of Remote Sensing, 2018, 39, 7547-7567.	1.3	5
51	IRG2018: A regional geoid model in Iran using Least Squares Collocation. Studia Geophysica Et Geodaetica, 2019, 63, 191-214.	0.3	5
52	Multiview Active Learning Optimization Based on Genetic Algorithm and Gaussian Mixture Models for Hyperspectral Data. IEEE Geoscience and Remote Sensing Letters, 2020, 17, 172-176.	1.4	5
53	Electrical and Dielectric Characteristics of SrTiO ₃ Thin Films Grown by PE-MOCVD Technique. Materials Research Society Symposia Proceedings, 1993, 335, 107.	0.1	4
54	A fast-adaptive support vector method for full-pixel anomaly detection in hyperspectral images. , 2011, ,		4

#	Article	IF	CITATIONS
55	Graph-based semi-supervised hyperspectral image classification using spatial information. , 2016, , .		4
56	Sparse Reconstruction of Regional Gravity Signal Based on Stabilized Orthogonal Matching Pursuit (SOMP). Pure and Applied Geophysics, 2016, 173, 2087-2099.	0.8	4
57	A computationally efficient multi-domain active learning method for crop mapping using satellite image time-series. International Journal of Remote Sensing, 2019, 40, 6383-6394.	1.3	3
58	A New Statistical Test Based on the WR for Detecting Offsets in GPS Experiment. Earth and Space Science, 2020, 7, e2019EA000810.	1.1	3
59	Development of a hybrid tomography model based on principal component analysis of the atmospheric dynamics and GPS tracking data. GPS Solutions, 2022, 26, 1.	2.2	3
60	Multiple kernels learning for classification of agricultural time series data. , 2014, , .		2
61	SPHEROIDAL SPLINE INTERPOLATION AND ITS APPLICATION IN GEODESY. Geodesy and Cartography, 2020, 46, 123-135.	0.2	2
62	ASSESSMENT OF OPTIMUM VALUE FOR DIP ANGLE AND LOCKING RATE PARAMETERS IN MAKRAN SUBDUCTION ZONE. International Archives of the Photogrammetry, Remote Sensing and Spatial Information Sciences - ISPRS Archives, 0, XLII-4/W4, 523-529.	0.2	2
63	CLUSTERING OF MULTI-TEMPORAL FULLY POLARIMETRIC L-BAND SAR DATA FOR AGRICULTURAL LAND COVER MAPPING. International Archives of the Photogrammetry, Remote Sensing and Spatial Information Sciences - ISPRS Archives, 0, XL-1/W5, 701-705.	0.2	2
64	Precise estimation of horizontal displacement by combination of multi-GNSS (Galileo and GPS) observations via the LS-VCE method. Applied Geomatics, 0, , 1.	1.2	2
65	MOCVD Growth of Epitaxial SrTiO3 Thin Films on YBa2 Cu3O7â^'x/LaAlO3. Materials Research Society Symposia Proceedings, 1993, 335, 113.	0.1	1
66	An efficient framework for spectral-spatial classification of hyperspectral images in urban areas. , 2014, , .		1
67	An improved marker selection method for hyperspectral image segmentation and classification. , 2014, , .		1
68	A special case of the Poisson PDE formulated for Earth's surface and its capability to approximate the terrain mass density employing land-based gravity data, a case study in the south of Iran. Geophysical Journal International, 2016, 207, 1529-1553.	1.0	1
69	Classifying Multi-Channel Polsar Images Base on Polarization Signature. , 2018, , .		1
70	Adaptive Self-Learned Active Learning Framework for Hyperspectral Classification. , 2019, , .		1
71	Single point positioning performance of single-frequency code-based mode with ionospheric modelling: a case study over Iran. Journal of Spatial Science, 2020, , 1-22.	1.0	1
72	A recovered Moho model by integrated inversion of gravity and seismic depths in Iran. Heliyon, 2020, 6, e03636.	1.4	1

#	Article	IF	CITATIONS
73	Multi-GNSS (CPS/Galileo) single-frequency precise point positioning: a case study over Victoria. Earth Science Informatics, 2021, 14, 1303-1313.	1.6	1
74	SEGMENTATION OF POLARIMETRIC SAR IMAGES USIG WAVELET TRANSFORMATION AND TEXTURE FEATURES. International Archives of the Photogrammetry, Remote Sensing and Spatial Information Sciences - ISPRS Archives, 0, XL-1/W5, 613-617.	0.2	1
75	GRAPH-BASED SEMI-SUPERVISED HYPERSPECTRAL IMAGE CLASSIFICATION USING SPATIAL INFORMATION. International Archives of the Photogrammetry, Remote Sensing and Spatial Information Sciences - ISPRS Archives, 0, XLII-4/W4, 91-96.	0.2	1
76	Establishment of a corrective geoid surface by spline approximation of Iranian GNSS/levelling network. Measurement: Journal of the International Measurement Confederation, 2022, , 111341.	2.5	1
77	Surface Smoothing Process of YBa2Cu3O7â^'x Thin Film for Fabrication of Superconducting Multi-Chip Modules. Materials Research Society Symposia Proceedings, 1993, 318, 665.	0.1	0
78	Performance Comparison of Contemporary Anomaly Detectors for Detecting Man-Made Objects in Hyperspectral Images. Photogrammetrie, Fernerkundung, Geoinformation, 2013, 2013, 19-30.	1.2	0
79	A numerical investigation into the ability of the Poisson PDE to extract the mass-density from land-based gravity data: A case study of salt diapirs in the north coast of the Persian Gulf. Journal of Applied Geophysics, 2017, 143, 50-61.	0.9	0
80	Estimation of Natural Hazard Damages through the Fusion of Change Maps Obtained from Optical and Radar Earth Observations. Proceedings (mdpi), 2018, 2, .	0.2	0
81	Ensemble Learning for Crop Monitoring from Multitemporal Optical and Synthetic Aperture Radar Earth Observations. , 2021, , .		Ο
82	EVALUATION OF MULTIPLE KERNEL LEARNING ALGORITHMS FOR CROP MAPPING USING SATELLITE IMAGE TIME-SERIES DATA. International Archives of the Photogrammetry, Remote Sensing and Spatial Information Sciences - ISPRS Archives, 0, XLII-4/W4, 201-207.	0.2	0
83	Combination of regional and global geoid models at continental scale: application to Iranian geoid. Annals of Geophysics, 2021, 64, GD434.	0.5	0